Trait-based food web model reveals the underlying mechanisms of biodiversity-ecosystem functioning relationships

Maureaud, Aurore; Andersen, Ken Haste; Zhang, Lai; Lindegren, Martin

Published in:
Journal of Animal Ecology

Link to article, DOI:
10.1111/1365-2656.13207

Publication date:
2020

Document Version
Peer reviewed version

Supporting Information

This document contains the supplementary material (additional methods and analyses) associated to the following article.

Title: Trait-based food web model reveals the underlying mechanisms of biodiversity-ecosystem functioning relationships

Authors: Maureaud Aurore[1], Ken H. Andersen[1], Lai Zhang[2], Martin Lindegren[1]

[1] Centre for Ocean Life, Technical University of Denmark, Kgs. Lyngby, Denmark
[2] School of Mathematical Science, Yangzhou University, Yangzhou 225002, China

Corresponding author: Aurore Maureaud, auma@aqua.dtu.dk

Appendix S1. Standardization on food web simulations.

The number of food webs assembled per species richness level is not evenly distributed (Fig. S1), and needs to be standardized to enable a comparison between ecosystem functions and BEF relationships across richness levels.

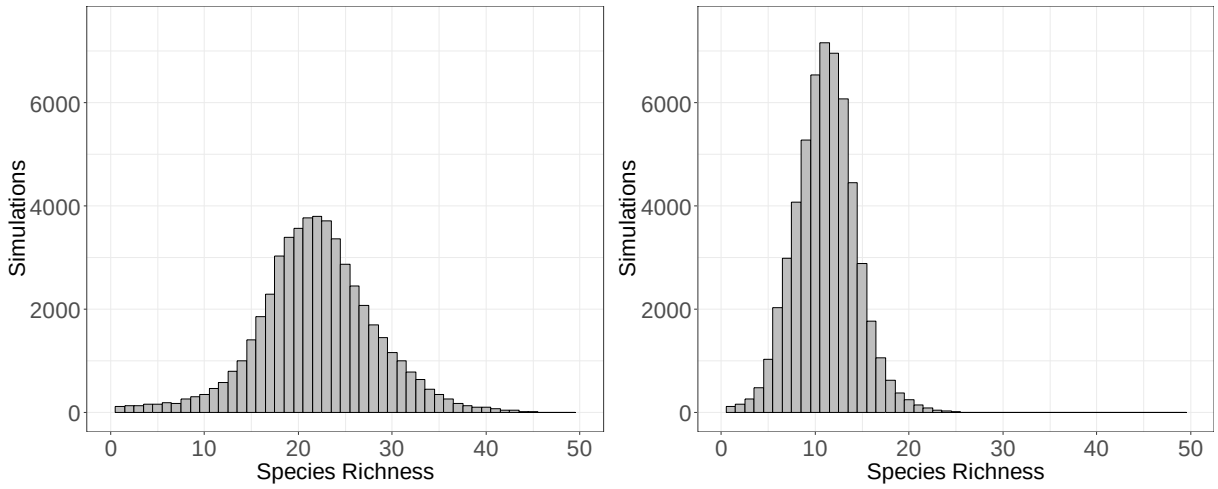

Figure S1: Distribution of the number of food web simulations for all runs against species richness for the simulations used in the main analysis where the home range parameter $\alpha = 0.5$ (left) and for the modified structure where the home range parameter $\alpha = 2$ (right).

For the first set of simulations ($\alpha = 0.5$), we obtained in total 50,673 food webs containing a maximum of 46 species. At each richness level we randomly selected 50 food webs to cover evenly the richness gradient from 1 to 40 species, resulting in a subset of 2200 food webs (Table S1). For the second set of simulations ($\alpha = 2$), we obtained 54,755 food webs containing a maximum of 26 species. Similarly, we randomly selected 50 food webs at each richness level and obtained 1100 food webs from 1 to 22 species. Those randomly selected food webs are used for the rest of the analyses of the study.

Table S1: Description of the number of simulations and community assemblies before and after standardization for each set of simulations.

Property	**Set of simulations**	
Home range coefficient	$\alpha = 0.5$	$\alpha = 2$
Number of community assemblies	100	100
Minimum number of species	1	1
Maximum number of species	46	26
Number of food webs	50,673	54,755
Number of food webs after standardization (per species richness level)	50	50
Number of food webs after standardization (total)	1100	2000

Appendix S2. Validation of the model

To verify if the assembled food webs reproduce patterns observed in natural food webs, we compared a suite of food web metrics and macroecological patters with empirical data. Such comparisons have been done previously for similar food web models (Hartvig, 2011; Ritterskamp, Bearup, & Blasius, 2016), however, those model also included processes that we ignored, such as ontogeny and functional responses (Hartvig, 2011) or interference competition and intraspecific competition/self-regulation (Ritterskamp et al., 2016). Therefore, we expect that our model under-estimates diversity of natural food webs. Overall, we find that our model simulations somewhat low diversity, however, the size-scaling of diversity and network metrics follow the empirical expectations. We therefore find that the model reproduces well empirical food webs.

We performed five main test, following the validation from Hartvig (2011): size-scaling of species richness, size-scaling of total biomass, connectance, maximum trophic level, and the correlation between number of links and number of species.

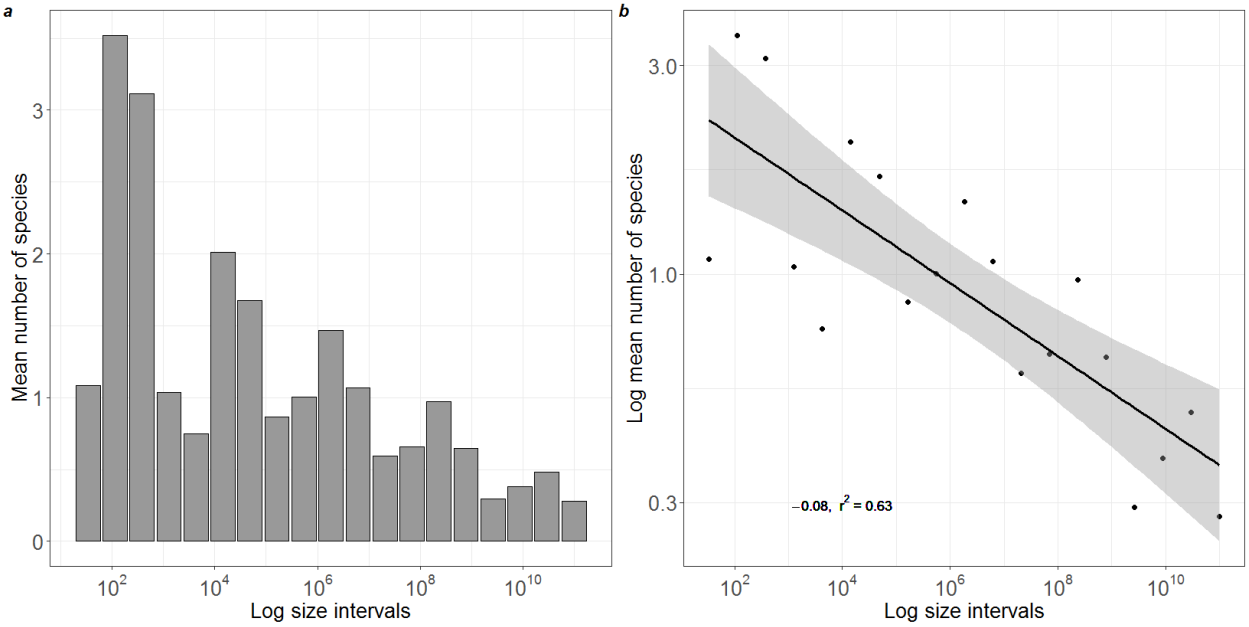

Figure S2.1: Size scaling of species richness: (a) Distribution of the number of species within log-size classes (b) and linear regression on log(m), log(mean number of species). The slope and the explained variance are indicated on the graph.

We checked the distribution of the number of species along the size trait by creating 20 log-intervals, evenly distributed along the size axis (Figure S2.1,a). The slope of the log-log relationship between species richness and size was -0.08 (Figure S2.1,b), which is outside of the empirical range -0.23 ± 0.07, where values are ranged between $[-0.33; +0.12]$ (Hartvig, 2011; Reuman, Mulder, Raffaelli, & Cohen, 2008). It seems that the slope is lower compared to

the model developed by (Hartvig, 2011) and we found fewer species in small size classes and more species in larger size classes.

Second, we checked the distribution of the mean biomass along the size trait, by again creating 20 log-intervals, evenly distributed along the size axis (Figure S2.2,a). Similarly, we conducted a linear regression on a log-log scale and found a slope of -0.14 (Figure S2.2,b), which is also within the empirical expected range (Sprules & Barth, 2016; Zhang, Hartvig, Knudsen, & Andersen, 2014).

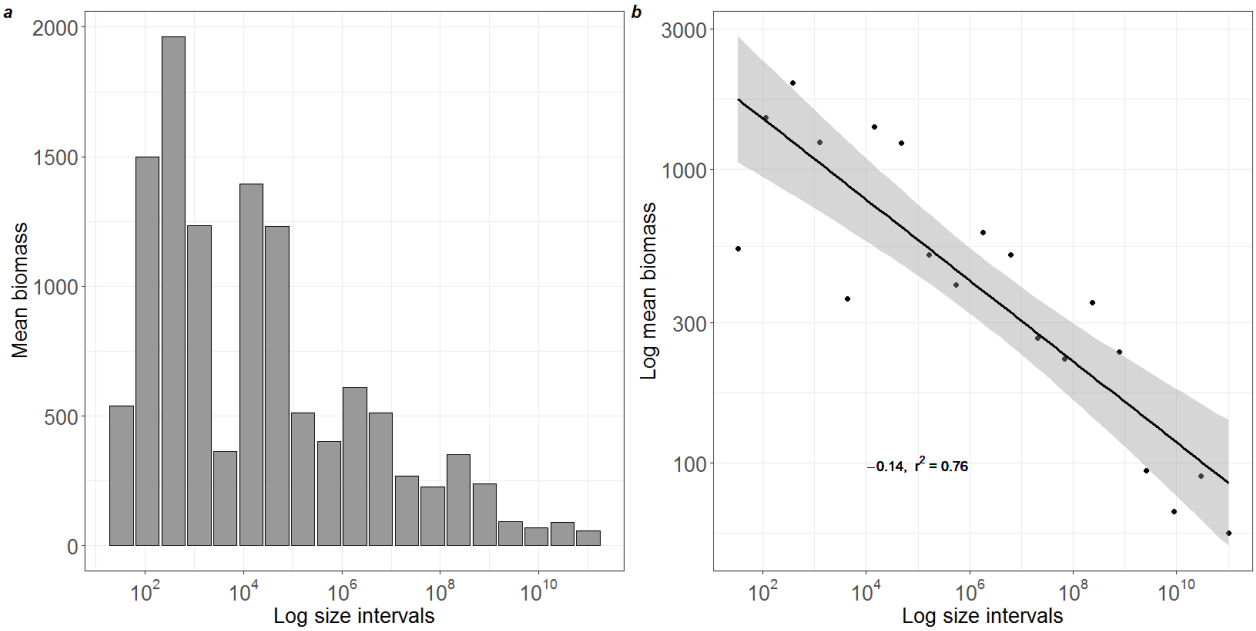

Figure S2.2: Size scaling of biomass: (a) Biomass distribution within log-size classes (b) and linear regression on log(m), log(mean biomass). The slope and the explained variance are indicated on the graph.

Third, we compared some network metrics between the simulated food webs with the trait-based model and empirical food web data (Hartvig, 2011; Rossberg, Ishii, Amemiya, & Itoh, 2008). Specifically, we compared the number of species obtained, the connectance and the food chain length. All metrics compared are within the empirical expected range (Table S2). However, this test is not very strong since the number of species in empirical food web is very variable. The distribution of the size scaling of the number of species is a better metric to strengthen the validation of the model. Similarly, the connectance is sensitive to the link threshold (Hartvig, 2011) in the model and sensitive to sampling in empirical food web. The food chain length, on the opposite, does not depend on the link threshold and is a more robust measure for comparing model simulations and empirical food webs.

Table S2: Comparison of network metrics between the model simulations and empirical food webs (Rossberg et al., 2008).

	Outputs from model	Empirical webs
Food webs analyzed	1950	17
Number of species	20 ± 11.5	54 ± 35
Connectance	0.19 ± 0.05	0.16 ± 0.10
Food chain length	5.88 ± 1.30	6.4 ± 4.1

Finally, we compared the number of established link in the food web with the number of species. This relationship follows a power-law curve: $L = aS^b$ where L is the number of links and S the number of species. We fitted a non-linear curve with the R function *nls* and estimated the parameter of interest and R^2 (Figure S2.3). The parameter b is expected to fall between 1 and 2, depending on the threshold applied to decide whether a link is established or not (Hartvig, 2011; Riede et al., 2010). Our results show a high parameter, because we chose a small threshold, and therefore b is closer to 2 than to 1.5 ($b = 1.97$).

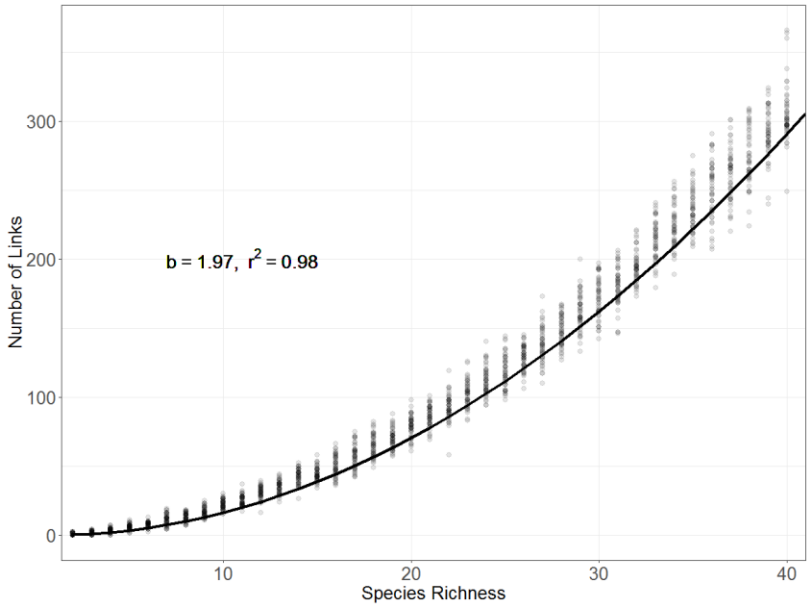

Figure S2.3: Relationship between the number of links and the number of species in 1950 food webs, randomly selected from all simulations.

Appendix S3. Sensitivity to parameter values

The results observed with this theoretical food web model also rely on the values of the parameters (described in Table 1). While we already performed a sensitivity analysis for the home range coefficient via the food web structure manipulation, we did not specifically test for the sensitivity of the other parameters.

Several resource capacity K values and species pool sizes have been tested and evaluated previously by Zhang et al. (2014). We selected a species pool large enough (200 species) to ensure that the length of the food chain is not influenced by the pool size and within a realistic range (see Appendix S2). On other hand, the resource carrying capacity has a stronger influence on the length of the food chain, and we ensured that the carrying capacity is sufficiently high to allow a food chain that was similar to observed natural food webs (see Appendix S2).

The width of the selection function σ_m and the preferred predator: prey mass ratio β, modifies the feeding preference and the limiting similarity along the trait axis. Thereby they have the potential of changing the diversity in the food web. Decreasing the width of the food selection σ_m lowers the similarity between species and makes it possible to pack more species in the range of the habitat axis. Lowering σ_m will therefore increase diversity. However, the scaling relationships we observe along the richness gradient are not expected to change in their shape.

The same argument applies for the preferred predator: prey mass ratio; lowering β gives less trophic overlap and therefore more trophic levels can be packed into the same size range. However, the number of trophic level will remain the same. The total impact on the structure and function will therefore be limited.

Similarly, the constant for intrinsic mortality c, the conversion efficiency ε and the resource intrinsic growth rate r are expected to change the amount of losses and production rate. For instance, we can expect metabolism to increase if c increases. We can expect predation loss to decrease if ε increases. Similarly, the production rate and productivity would increase if r increases. Although the manipulation of those parameters can change the absolute values of the ecosystem functions, we foresee that they would scale similarly with diversity and food web structure.

Although the choice of the fixed parameters in the food web might slightly change the observed relationships, but mainly the absolute values of diversity/ecosystem functions, we do not expect that they would modify the overall patterns observed.

Appendix S4. The trait space.

Figure S4.2 shows two food webs with low and high number of species. These food webs are assembled following equations in Table 2 in the main analysis. The equation that quantifies the percentage of the filled trait space requires a threshold that indicates whether a grid cell in the trait space is filled by the species interaction strength or not. Several values of that threshold have been tested and results are shown in Figure S4.2. We selected a threshold high enough to ensure that the curve is representative of the trait completeness (0.001).

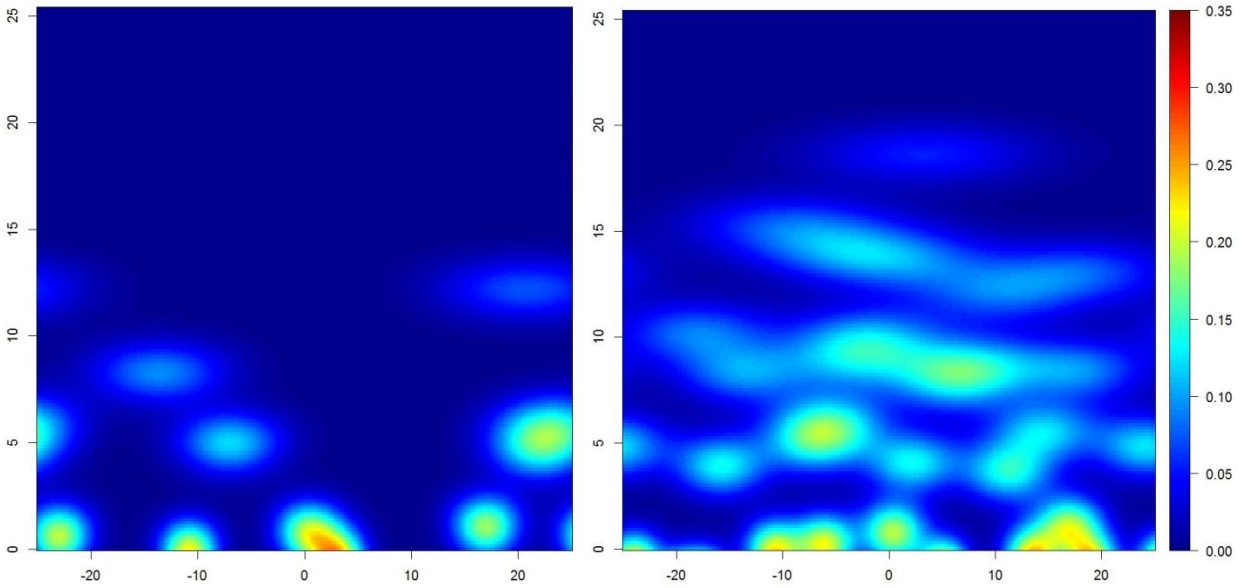

Figure S4.1: Surface plots of the filled trait space for 10 species food web (left) and 30 species food web (right) where the color corresponds to the sum of the interaction coefficients of all the species for all the cells in the trait space. y-axis: log(body size), x-axis: habitat trait.

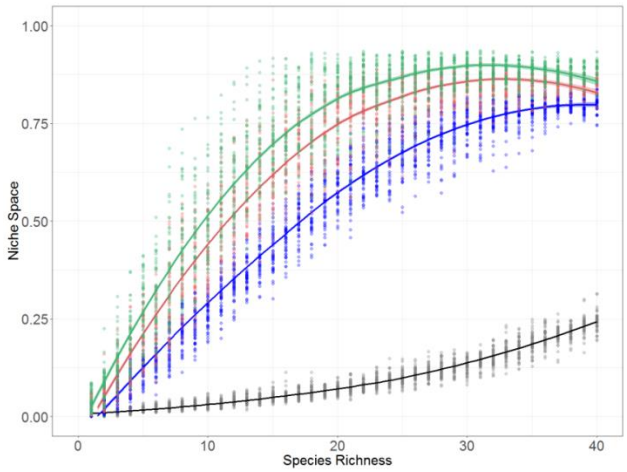

Figure S4.2: Proportion of trait space filled against species richness for different threshold values (in grey: 0.1, in blue: 0.01, in red: 0.001, in green: 0.0001). Each line is a smooth based on the threshold value of the same color.

Appendix S5. Shapes of richness-ecosystem functioning relationships.

In order to investigate the differences in the shapes of the richness-ecosystem functioning relationships, we fitted non-linear functions following Michaelis-Menten curves to explain the ecosystem function *F*:

$$F(x) = \frac{a\,x}{b + x} \quad \text{(S4.1)}$$

We also fitted power law curves and compared the fits:

$$F(x) = ax^b \quad \text{(S4.2)}$$

In one case, a linear curve also seemed appropriate:

$$F(x) = ax + b \quad \text{(S4.3)}$$

Finally, we also tried sigmoidal curves:

$$F(x) = \frac{a}{1 + be^{-cx}} \quad \text{(S4.4)}$$

The results of the mathematical linear and non-linear fits are detailed below in Figure S5.1 and Table S5.1. We chose the best model based on highest explained variance and lowest Akaike Criterion. Two models are considered different if $\Delta AIC > 2$. Therefore we conclude on the shape of the different richness-function relationships:

- Richness-Biomass is best fitted by a sigmoidal curve
- Richness-Metabolism is best fitted by a sigmoidal curve
- Richness-Production is best fitted by a Michaelis-Menten curve
- Richness-Productivity is best fitted by a sigmoidal curve

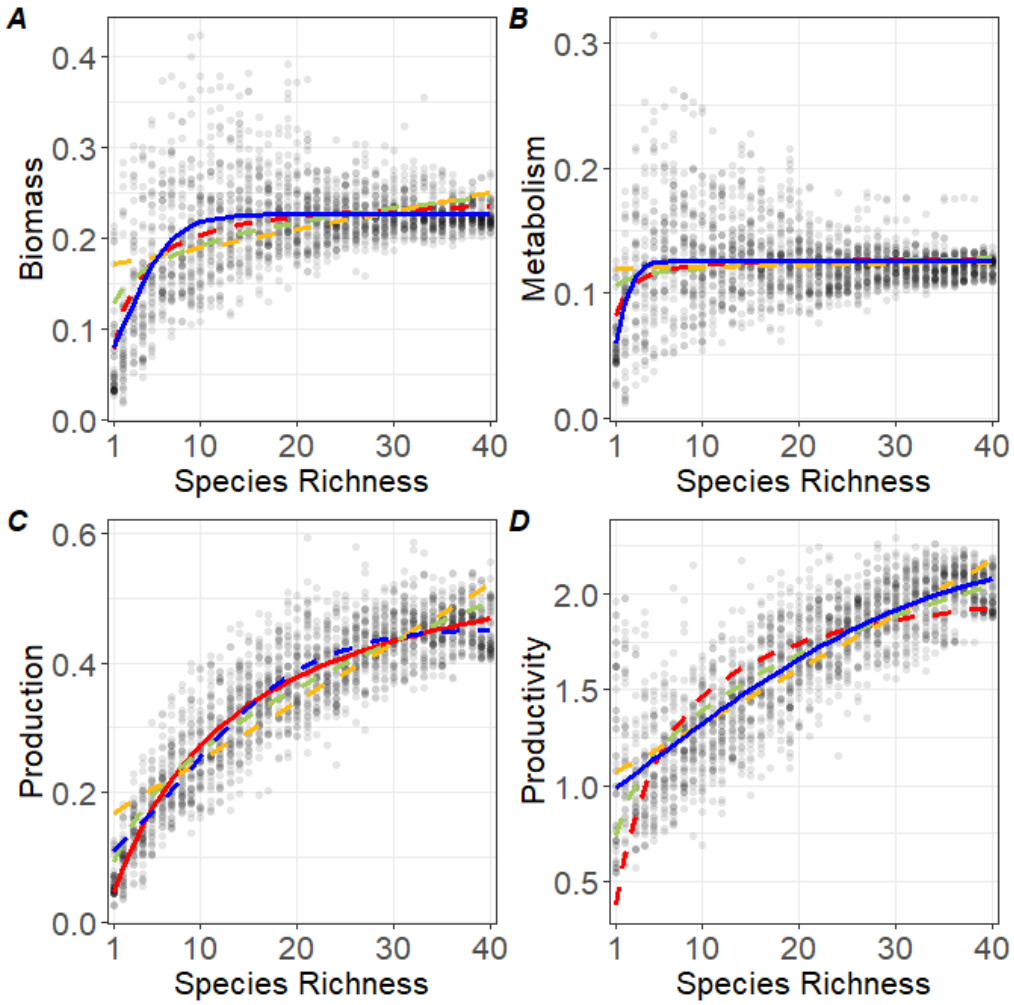

Figure S5.1: Results from the mathematical fits on each biodiversity-function relationship for the set of simulations where $\boldsymbol{\alpha = 0.5}$: A) Biomass, B) Metabolism, C), Production and D) Productivity. Lines represent the mathematical curves: Michaelis-Menten (red), Power (green), Linear (orange), Sigmoidal (blue). Solid lines represent the best model selected based on AIC and r-squared.

Table S5.1: Description of mathematical fits for each richness-function relationship for the set of simulations where $\alpha = 0.5$. R2 is the explained variance and AIC is the Akaike criterion value. Lines in bold represent the best model fit based on R2 and AIC values. Grey colored cells represent the best fitted mathematical curve for each relationship.

Function	Model	Parameter	Value	R2	AIC
Biomass	**Michaelis-Menten**	a	0.25	0.39	-6770
		b	2.34		
	Power	a	0.13	0.32	-6543
		b	0.19		
	Linear	a	0.00	0.19	-6208
		b	0.17		
	Sigmoidal	a	0.23	**0.40**	**-6804**
		b	2.21		
		c	0.33		
Metabolism	**Michaelis-Menten**	a	0.13	0.11	-8510
		b	0.66		
	Power	a	0.10	0.05	-8377
		b	0.06		
	Linear	a	0.00	0.01	-8296
		b	0.12		
	Sigmoidal	a	0.13	**0.14**	**-8568**
		b	2.36		
		c	0.90		
Production	**Michaelis-Menten**	a	0.63	**0.85**	**-6434**
		b	13.08		
	Power	a	0.09	0.83	-6225
		b	0.46		
	Linear	a	0.01	0.75	-5502
		b	0.16		
	Sigmoidal	a	0.46	0.84	-6389
		b	3.83		
		c	0.16		
Productivity	**Michaelis-Menten**	a	2.12	0.52	428
		b	4.49		
	Power	a	0.74	0.67	-339
		b	0.27		
	Linear	a	0.03	0.70	-518
		b	1.04		
	Sigmoidal	a	2.32	**0.71**	**-602**
		b	1.41		
		c	0.06		

We repeated this method to compare the richness-ecosystem functioning relationships between communities with a high home range coefficient (Figure S5.2 and Table S5.2). We conclude on the shape of the different richness-function relationships:

- Richness-Biomass is best equally fitted by Michaelis-Menten and sigmoidal mathematical curves
- Richness-Metabolism is best fitted by a Michaelis-Menten mathematical curve
- Richness-Production is best fitted by a sigmoidal mathematical curve
- Richness-Productivity is best fitted by a sigmoidal mathematical curve

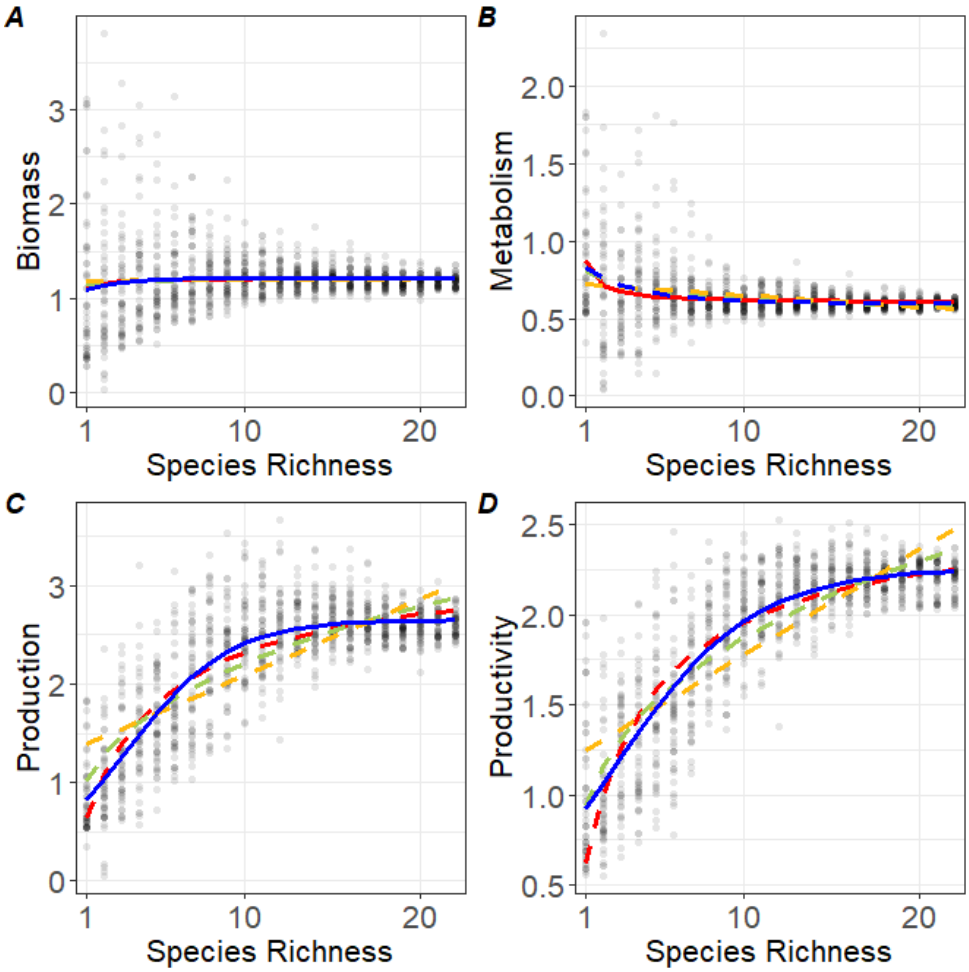

Figure S5.2: Results from the mathematical fits on each biodiversity-function relationship for the set of simulations where $\boldsymbol{\alpha = 2}$: A) Biomass, B) Metabolism, C), Production and D) Productivity. Lines represent the mathematical curves: Michaelis-Menten (red), Power (green), Linear (orange), Sigmoidal (blue). Solid lines represent the best model selected based on AIC and r-squared.

We observe a decreasing relationship between metabolism and richness, where metabolism is higher under low levels of richness (Figure S5.2B and Table S5.2). This may be due to small

species (small value on the size axis), lacking predation. In the model, metabolism is lower for large species so dominance of small species may promote higher metabolism compared to species rich food webs.

Table S5.2: Description of mathematical fits for each richness-function relationship for the set of simulations where $\alpha = 2$. R2 is the explained variance and AIC is the Akaike criterion value. Lines in bold represent the best model fit based on R2 and AIC values. Grey colored cells represent the best fitted mathematical curve for each relationship.

Function	Model	Parameter	Value	R2	AIC
Biomass	**Michaelis-Menten**	a	1.22	**0.005**	**838**
		b	0.11		
	Power	a	1.15	0.002	841
		b	0.02		
	Linear	a	0.00	0.003	843
		b	1.19		
	Sigmoidal	a	1.21	**0.006**	**838**
		b	0.19		
		c	0.57		
Metabolism	**Michaelis-Menten**	a	0.60	**0.09**	**-609**
		b	-0.31		
	Power	a	0.81	**0.09**	**-607**
		b	-0.11		
	Linear	a	-0.01	0.06	-575
		b	0.73		
	Sigmoidal	a	0.59	0.09	-604
		b	-0.35		
		c	0.25		
Production	**Michaelis-Menten**	a	3.26	0.68	1019
		b	4.05		
	Power	a	1.01	0.64	1146
		b	0.34		
	Linear	a	0.08	0.53	1426
		b	1.31		
	Sigmoidal	a	2.65	**0.70**	**934**
		b	3.16		
		c	0.35		
Productivity	**Michaelis-Menten**	a	2.58	0.71	88
		b	3.16		
	Power	a	0.94	0.72	47
		b	0.30		
	Linear	a	0.06	0.64	341
		b	1.19		
	Sigmoidal	a	2.26	**0.76**	**-97**
		b	1.86		
		c	0.25		

Appendix S6. Relationships between multiple ecosystem functioning metrics and their statistical trade-offs.

We investigated the correlation and multidimensional relationships between the ecosystem functioning metrics (Figure S6.1). Biomass is indeed much related to metabolism, and production and productivity are also strongly correlated. However, the correlation between biomass and productivity is low (0.16), just as the correlation between metabolism and productivity (-0.14).

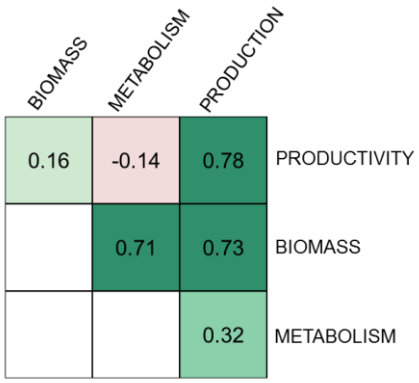

Figure S6.1: Correlation panel between the four metrics of ecosystem functioning included in the main analysis (green is positive and red is negative).

The Principle Component Analysis also confirms this and suggests that some communities are not able to maximize several functions simultaneously, where they would exhibit high productivity but low metabolism for instance (Figure S6.2).

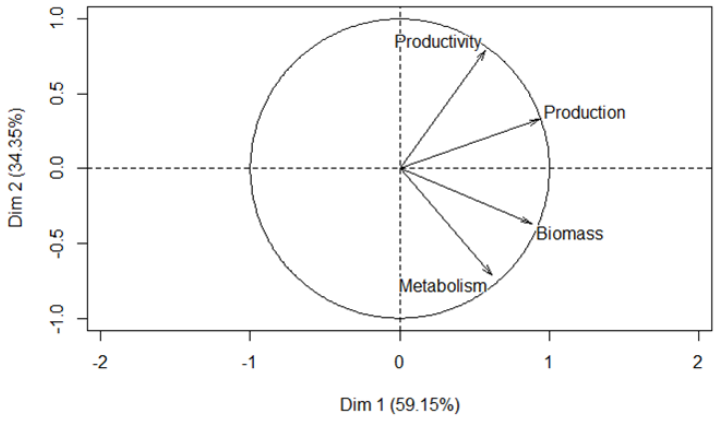

Figure S6.2: Principle Component Analysis based on all simulations and the four ecosystems functioning metrics. The percentage indicates how much of the variability is captured by dimensions 1 and 2.

This would indicate the existence of trade-offs in communities. However, communities with high biomass would be likely to exhibit also high metabolism and production, indicating the existence of synergies.

Additionally, we show that high productivity is linked to high predation loss per species or per food web (Figure S6.3), accelerating the transfer of energy is food webs. Communities dominated by metabolism losses remain longer in food webs and productivity is lower.

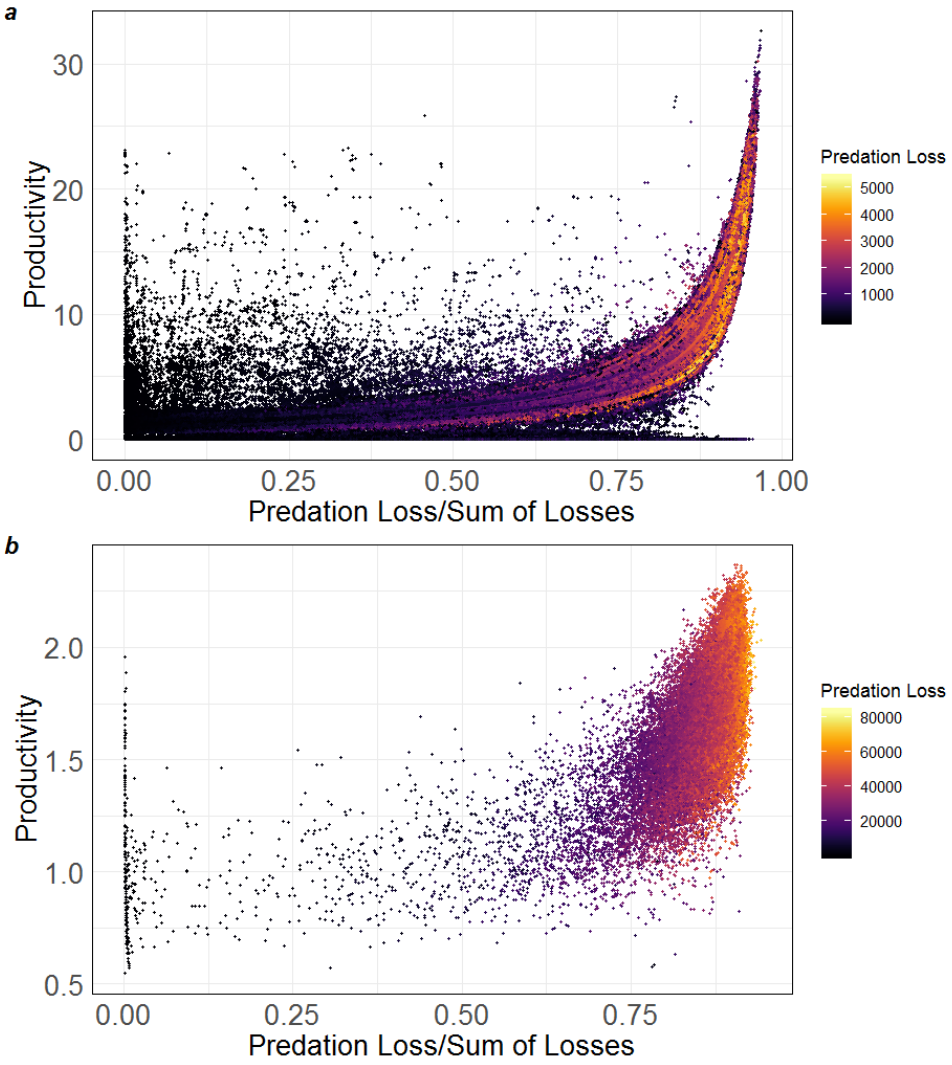

Figure S6.3: Productivity is higher when predation losses dominate energy loss for species (a) and food webs (b).

Appendix S7. Additional explanation on variance partitioning analyses.

Relationships between each ecosystem function and predictors included in the variance partitioning model were investigated beforehand. This allowed including non-linear effects by integrating squared-transformed terms, applying the following transformation to predictor X: $X' = (X - \bar{X})^2$, to avoid collinearity between X and X'. We tested multiple non-linear effects but only kept the ones improving the total variance explained, or changing the shared variance in the models. We always incorporated a non-linear term for species richness S, since all relationships are non-linear between species richness and ecosystem functions (see Appendix S5). We applied this transformation also for the number of top-predators T_p to explain metabolism; for the maximum proportion D_1 to explain production and productivity. This results in the following models:

$$F \sim [X_1] + [X_2] + [X_2] + [X_4]$$

$$B \sim [D_1 + D_2 + D_3] + [S + (S - \bar{S})^2] + \left[\tau_{max} + \tau_{mean} + C + T_p\right] + \left[T_{space}\right]$$

$$M \sim [D_1 + D_2 + D_3] + [S + (S - \bar{S})^2] + \left[\tau_{max} + \tau_{mean} + C + T_p + (T_p - \overline{T_p})^2\right] + \left[T_{space}\right]$$

$$P \sim [D_1 + (D_1 - \overline{D_1})^2 + D_2 + D_3] + [S + (S - \bar{S})^2] + \left[\tau_{max} + \tau_{mean} + C + T_p\right] + \left[T_{space}\right]$$

$$Q \sim [D_1 + (D_1 - \overline{D_1})^2 + D_2 + D_3] + [S + (S - \bar{S})^2] + \left[\tau_{max} + \tau_{mean} + C + T_p\right] + \left[T_{space}\right]$$

The variance partitioning analysis allows quantifying the simultaneous importance of drivers from different groups, quantifying which predictors act as single drivers or not (Figure S7 and Table S7).

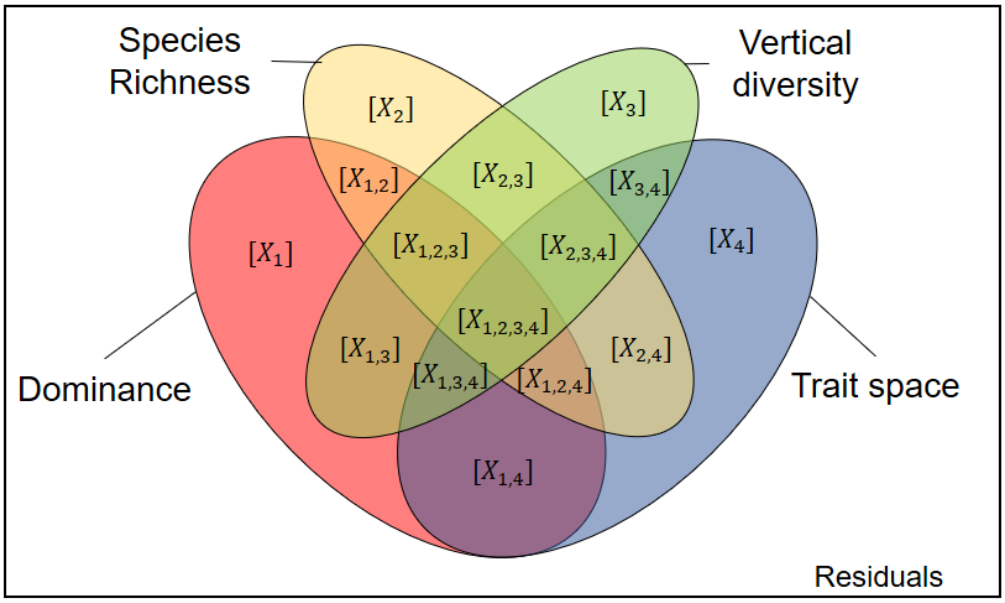

Figure S7: Variance partitioning and illustration of each possible combination of drivers. Variables $\boldsymbol{X_1, X_2, X_3, X_4}$ represent the 4 groups of explanatory variables (dominance, species richness, vertical diversity and trait space, respectively). The background white frame represents any residual variability unexplained by the explanatory variables.

Table S7: Results from the variance partitioning analyses on each ecosystem function (biomass, metabolism, production and productivity). Variables $\boldsymbol{X_1, X_2, X_3, X_4}$ represent the 4 groups of explanatory variables (dominance, species richness, vertical diversity and trait space, respectively).

Driver	**R squared Biomass**	**R squared Metabolism**	**R squared Production**	**R squared Productivity**
X_1	0.49	0.37	0.056	0.042
X_2	<0.01	0.033	0.034	0.020
X_3	<0.01	0.20	0.024	0.047
X_4	<0.01	<0.01	<0.01	0.022
$X_1 + X_2$	0.014	0.014	0.020	0.040
$X_1 + X_3$	0.066	0.17	<0.01	0.039
$X_1 + X_4$	0.060	<0.01	<0.01	0.029
$X_2 + X_3$	<0.01	<0.01	0.014	0.017
$X_2 + X_4$	<0.01	<0.01	<0.01	<0.01
$X_3 + X_4$	<0.01	0.056	<0.01	<0.01
$X_1 + X_2 + X_3$	<0.01	<0.01	0.015	0.068
$X_1 + X_2 + X_4$	0.026	0.032	<0.01	<0.01
$X_1 + X_3 + X_4$	<0.01	<0.01	<0.01	<0.01
$X_2 + X_3 + X_4$	0.016	<0.01	0.013	0.011
$X_1 + X_2 + X_3 + X_4$	0.22	<0.01	0.72	0.57

Appendix S8. Dominance occurs because of species configurations in the trait space.

We wanted to understand how dominance occurs in food web. We hypothesized that dominance of one species is related to high consumption levels, low predation consumption from predators, or a combination of both, causing some species to become more abundant than others. Figure S8 shows that species high consumption levels represent high biomass no matter what the strength of the predation they experience. However, the highest biomass results of a combination of high consumption rates and low predation on species.

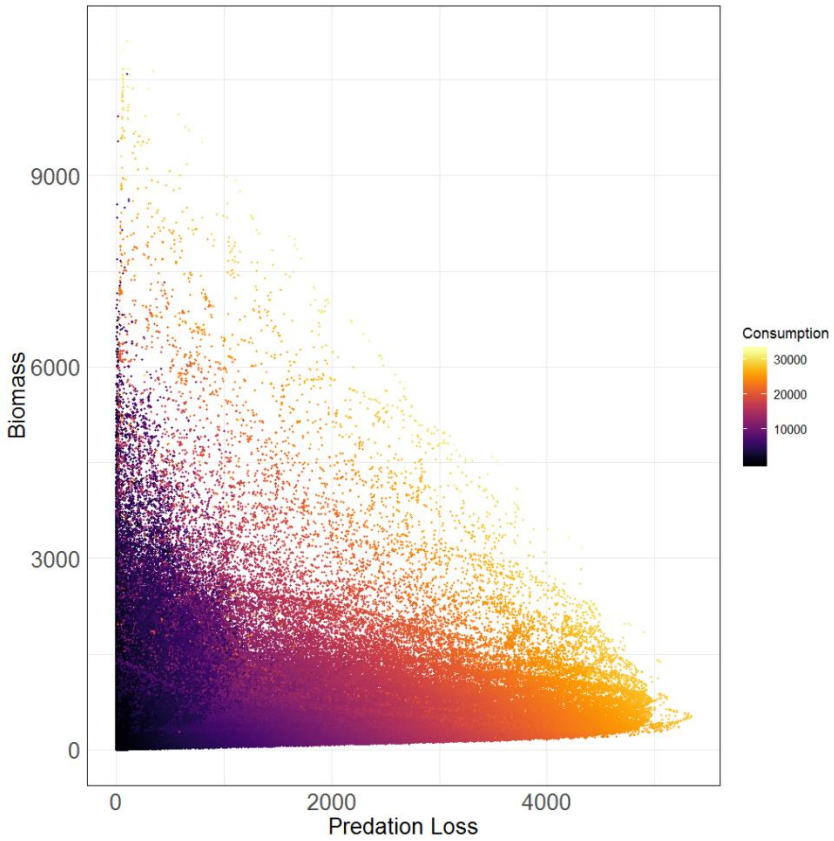

Figure S8: Relationship between biomass and predation loss. Each point on the scatter plot is a species, where the x-axis is the predation loss experienced by that species, its biomass on the y-axis and the color scale shows the consumption rate per species.

Appendix S9. Differences in biodiversity, network metrics, and ecosystem functioning in communities with low and high home range coefficients.

Our results show that connectance is lower when communities are characterized by a lower home range coefficient (Figures S9.1 and S9.2). Also, the mean trophic level reached by communities with a high home range is higher, probably caused by a more diversified diet allowed by a higher number of predation links established in the food web.

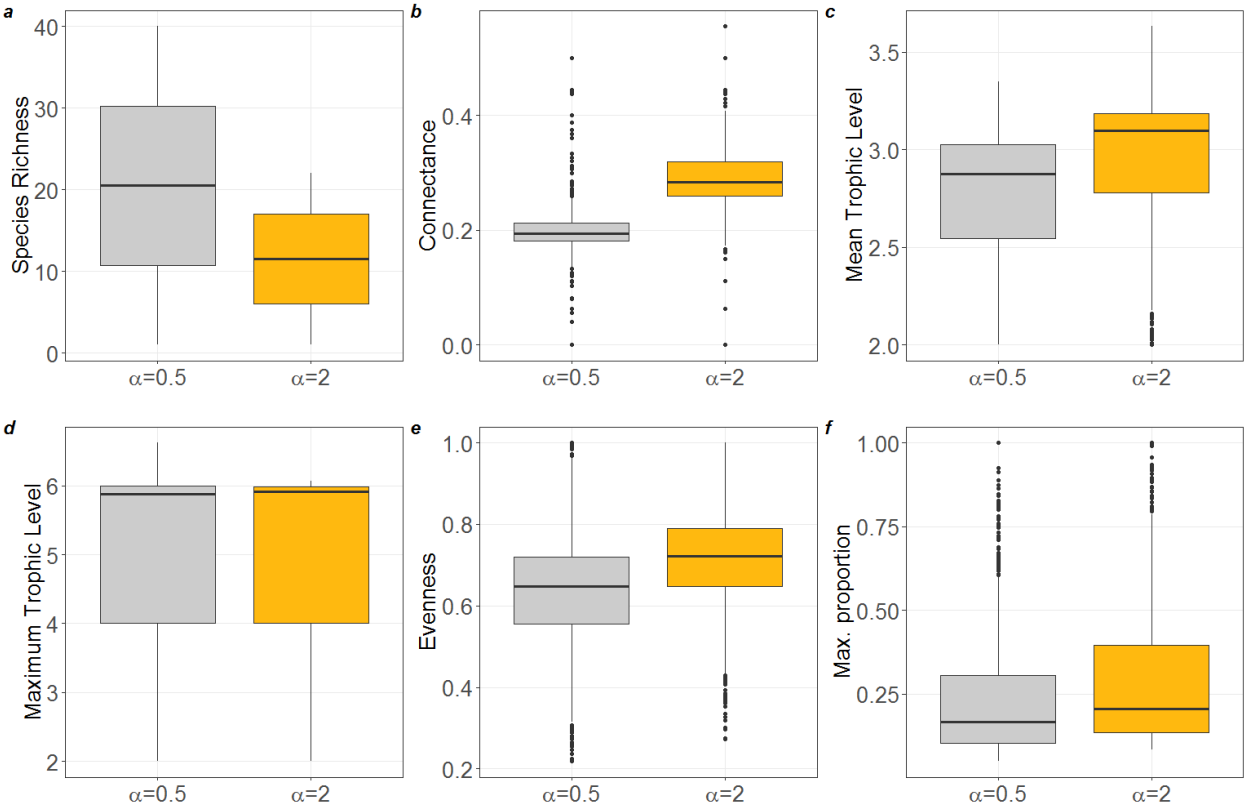

Figure S9.1: Comparison of the distribution of: (a) species richness, (b) connectance, (c) mean trophic level, (d) maximum trophic level (see equation in Table S1), (e) and Simpson´s evenness, and (f) maximum proportion of biomass allocated to one species; between communities with a low home range coefficient (in grey) and communities with a high home range (in yellow). All simulations are included.

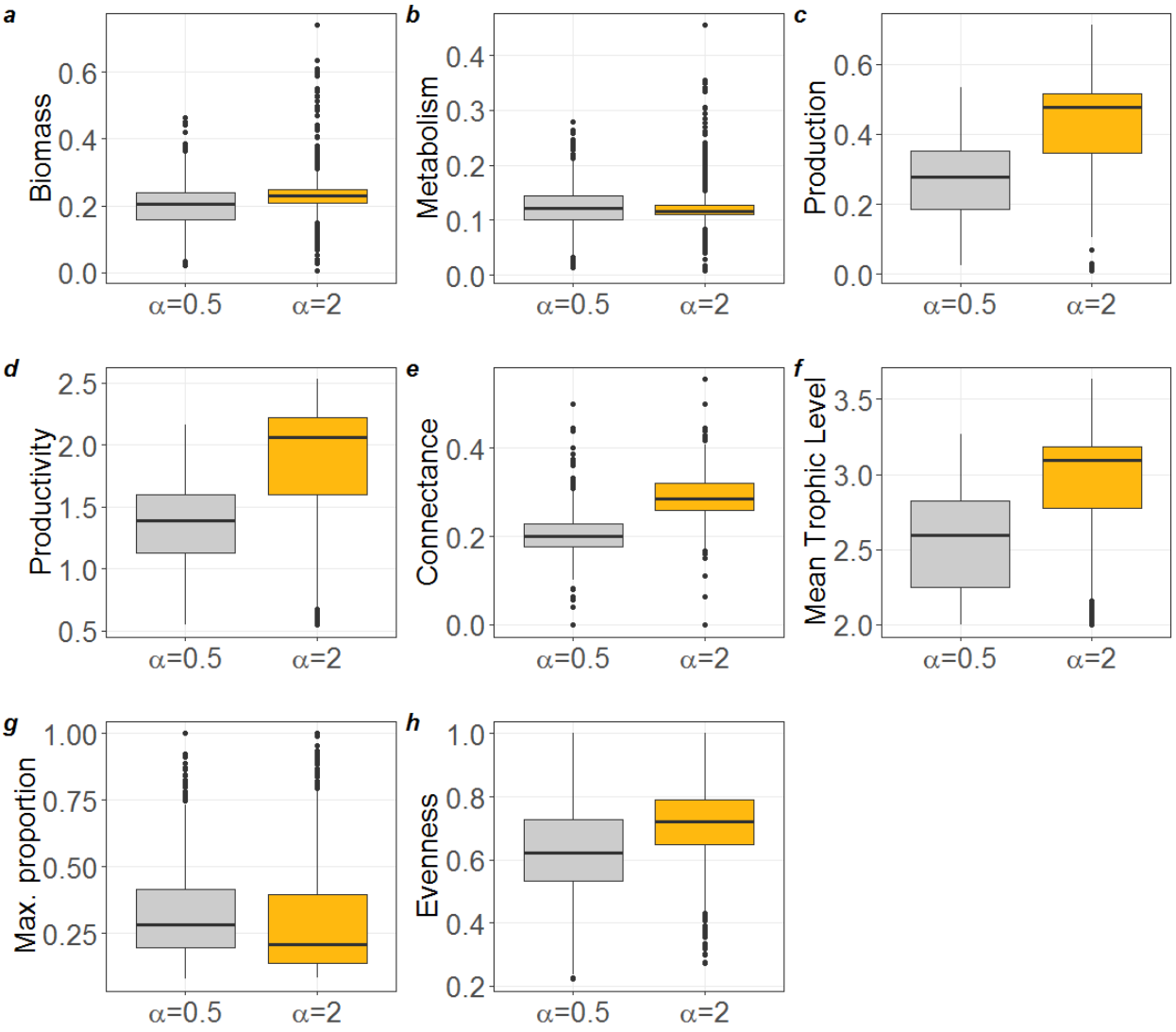

Figure S9.2: Comparison of the distribution of: (a) biomass, (b) metabolism, (c) production, (d) productivity, (e) connectance, (f) mean trophic level, (g) maximum proportion of biomass allocated to one species (h) and Simpson´s evenness between communities with a low home range coefficient (in grey) and communities with a high home range (in yellow). Only simulations from 1 to 20 species are included to compare similar richness levels.

References

Hartvig, M. (2011). *Food web ecology: individual life-histories and ecological processes shape complex communities*. Lund: Univ., Dept. of Biology.

Reuman, D. C., Mulder, C., Raffaelli, D., & Cohen, J. E. (2008). Three allometric relations of population density to body mass: theoretical integration and empirical tests in 149 food webs: Food web density-body mass relationships. *Ecology Letters*, *11*(11), 1216–1228. doi: 10.1111/j.1461-0248.2008.01236.x

Riede, J. O., Rall, B. C., Banasek-Richter, C., Navarrete, S. A., Wieters, E. A., Emmerson, M. C., … Brose, U. (2010). Scaling of Food-Web Properties with Diversity and Complexity Across Ecosystems. In *Advances in Ecological Research* (Vol. 42, pp. 139–170). doi: 10.1016/B978-0-12-381363-3.00003-4

Ritterskamp, D., Bearup, D., & Blasius, B. (2016). A new dimension: Evolutionary food web dynamics in two dimensional trait space. *Journal of Theoretical Biology*, *405*, 66–81. doi: 10.1016/j.jtbi.2016.03.042

Rossberg, A. G., Ishii, R., Amemiya, T., & Itoh, K. (2008). THE TOP-DOWN MECHANISM FOR BODY-MASS–ABUNDANCE SCALING. *Ecology*, *89*(2), 567–580. doi: 10.1890/07-0124.1

Sprules, W. G., & Barth, L. E. (2016). Surfing the biomass size spectrum: some remarks on history, theory, and application. *Canadian Journal of Fisheries and Aquatic Sciences*, *73*(4), 477–495. doi: 10.1139/cjfas-2015-0115

Zhang, L., Hartvig, M., Knudsen, K., & Andersen, K. H. (2014). Size-based predictions of food web patterns. *Theoretical Ecology*, *7*(1), 23–33. doi: 10.1007/s12080-013-0193-5